European Radiology (2019) 29:299–308
https://doi.org/10.1007/s00330-018-5584-y

UROGENITAL

Twelve-month prostate volume reduction after MRI-guided transurethral ultrasound ablation of the prostate

David Bonekamp[1] · M. B. Wolf[1] · M. C. Roethke[1] · S. Pahernik[2] · B. A. Hadaschik[2] · G. Hatiboglu[2] · T. H. Kuru[2] · I. V. Popeneciu[2] · J. L. Chin[3] · M. Billia[3] · J. Relle[4] · J. Hafron[4] · K. R. Nandalur[5] · R. M. Staruch[6] · M. Burtnyk[6] · M. Hohenfellner[2] · H.-P. Schlemmer[1]

Received: 8 January 2018 / Revised: 8 May 2018 / Accepted: 1 June 2018 / Published online: 25 June 2018

Abstract

Purpose To quantitatively assess 12-month prostate volume (PV) reduction based on T2-weighted MRI and immediate post-treatment contrast-enhanced MRI non-perfused volume (NPV), and to compare measurements with predictions of acute and delayed ablation volumes based on MR-thermometry (MR-t), in a central radiology review of the Phase I clinical trial of MRI-guided transurethral ultrasound ablation (TULSA) in patients with localized prostate cancer.

Materials and methods Treatment day MRI and 12-month follow-up MRI and biopsy were available for central radiology review in 29 of 30 patients from the published institutional review board-approved, prospective, multi-centre, single-arm Phase I clinical trial of TULSA. Viable PV at 12 months was measured as the remaining PV on T2-weighted MRI, less 12-month NPV, scaled by the fraction of fibrosis in 12-month biopsy cores. Reduction of viable PV was compared to predictions based on the fraction of the prostate covered by the MR-t derived acute thermal ablation volume (ATAV, 55°C isotherm), delayed thermal ablation volume (DTAV, 240 cumulative equivalent minutes at 43°C thermal dose isocontour) and treatment-day NPV. We also report linear and volumetric comparisons between metrics.

Results After TULSA, the median 12-month reduction in viable PV was 88%. DTAV predicted a reduction of 90%. Treatment day NPV predicted only 53% volume reduction, and underestimated ATAV and DTAV by 36% and 51%.

Conclusion Quantitative volumetry of the TULSA phase I MR and biopsy data identifies DTAV (240 CEM43 thermal dose boundary) as a useful predictor of viable prostate tissue reduction at 12 months. Immediate post-treatment NPV underestimates tissue ablation.

Key Points

- *MRI-guided transurethral ultrasound ablation (TULSA) achieved an 88% reduction of viable prostate tissue volume at 12 months, in excellent agreement with expectation from thermal dose calculations.*
- *Non-perfused volume on immediate post-treatment contrast-enhanced MRI represents only 64% of the acute thermal ablation volume (ATAV), and reports only 60% (53% instead of 88% achieved) of the reduction in viable prostate tissue volume at 12 months.*
- *MR-thermometry-based predictions of 12-month prostate volume reduction based on 240 cumulative equivalent minute thermal dose volume are in excellent agreement with reduction in viable prostate tissue volume measured on pre- and 12-month post-treatment T2w-MRI.*

Keywords High-intensity focused ultrasound ablation · Prostate cancer · Interventional magnetic resonance imaging · Thermometry · Biopsy, needle

✉ David Bonekamp
d.bonekamp@dkfz-heidelberg.de

[1] Department of Radiology (E010), German Cancer Research Center (DKFZ), Im Neuenheimer Feld 280, 69120 Heidelberg, Germany

[2] Department of Urology, University Hospital Heidelberg, Heidelberg, Germany

[3] Department of Urology, University of Western Ontario (UWO), London Health Sciences Center, Victoria Hospital, London, ON, Canada

[4] Department of Urology, Beaumont Health System, Royal Oak, MI, USA

[5] Department of Radiology, Beaumont Health System, Royal Oak, MI, USA

[6] Clinical Science, Profound Medical Inc., Toronto, ON, Canada

Abbreviations

AS	Active surveillance
ATAV	Acute thermal ablation volume
DSC	Dice similarity coefficient
DTAV	Delayed thermal ablation volume
MR-t	MR-thermometry
MRI	Magnetic resonance imaging
NPV	Non-perfused volume
PCa	Prostate cancer
PSA	Prostate-specific antigen
PV	Prostate volume
RPE	Radical prostatectomy
TULSA	Transurethral ultrasound ablation
UA	Ultrasound applicator

Introduction

In the developed world, prostate cancer (PCa) is the most commonly diagnosed solid cancer among men, and remains a leading cause of cancer death [1]. Prostate-specific antigen (PSA) screening has shifted many diagnoses towards low-grade PCa [2]. For patients with presumed clinically insignificant disease, traditional treatment options such as radical prostatectomy (RP) and whole-gland radiotherapy are associated with undue risk of side effects [3]. Conversely, while active surveillance (AS) can spare or delay the morbidity of treatment [4, 5], patient selection for AS is not optimal and a published 15-year follow-up study demonstrated that more than half of AS patients eventually undergo radical treatment [5].

Situations where the patient's decision for RP or AS is marginal call for minimally invasive treatments capable of achieving local disease control with a more favourable side-effect profile. Of several minimally invasive ablative treatments [6–13], prostate HIFU is the best evaluated [14]. However, HIFU is typically performed using transrectal ultrasound monitoring [15], which has limited ability to assess conformal treatment of targeted tissue and treatment boundaries. Live MRI monitoring during thermal therapy procedures has the potential to reduce over- or under-treatment by precisely localizing prostate cancer as demonstrated in MRI-guided biopsy [16–20], by providing real-time quantitative temperature measurement using MR thermometry (MR-t) [21] for treatment control and thermal dosimetry [6, 13, 22, 23], and by facilitating immediate post-treatment contrast-enhanced imaging for evaluation of treatment effect.

MRI-guided transurethral ultrasound ablation (TULSA) is a minimally invasive ablation technique that uses real-time MR-t to directly monitor and actively control treatment-relevant thermal energy deposition in an automated feedback algorithm, for conformal ablation of targeted prostate tissue [24–26]. MRI-guided TULSA has been evaluated in a prospective, multi-centre, safety and feasibility Phase I study for localized prostate cancer [26]. The published study included treatment-day volumetric measurement of the prostate, and assessment of linear precision and accuracy of the agreement between the treatment planning volume (boundary within which treatment is intended) and the thermometric isocontour recorded during the procedure at which at least 55° Celsius is reached, the acute target ablation volume (ATAV). Assessment of immediate post-procedure contrast-enhanced MRI (CE-MRI) allowing the determination of non-perfused volume (NPV) and 12-month MRI was only performed qualitatively.

The purpose of this study was to perform a quantitative analysis of viable prostate tissue volume reduction at 12 months after MRI-guided TULSA using T2-weighted MRI corrected for the previously unreported degree of fibrosis in biopsy cores, with a comparison with treatment-day predictors of ablation extent. This analysis quantitatively assessed if 12-month volume reduction confirmed predictions of viable tissue ablation by immediate post-treatment NPV, MR-t derived ATAV and delayed target ablation volume (DTAV) derived from MR-t calculations of thermal dose.

Materials and methods

Patients and TULSA technique

Details of the Phase I TULSA trial have been reported previously in Chin et al [26]. Briefly, it was a prospective, multi-centre, single-arm Phase I clinical trial of the safety and feasibility of prostate ablation in patients with localized PCa (NCT01686958, DRKS00005311). The study was ethics-approved and performed at three tertiary referral centres, with written informed consent from all patients. Thirty patients were included between March 2013 and March 2014, aged ≥ 65 years, presenting with biopsy-proven organ-confined PCa, clinical stage T1c-T2a (N0, M0), PSA ≤ 10 ng/ml, Gleason score (GS) 3+3 (n=24) or 3+4 (n=6), and no prior PCa treatment. Patients underwent MRI-guided TULSA, followed immediately with a post-interventional CE-MRI, and at 12 months underwent follow-up 12-core transrectal ultrasound-guided biopsy and MRI. MRI was performed using 3T MRI systems (Magnetom Trio, Siemens, Erlangen, Germany) with posterior and anterior multi-channel phased-array coils, using sequences described in Table 1. Biopsy data were processed at a central laboratory (Bostwick Laboratories, Glen Allen, VA, USA), with individual cores quantified for the length and percentage of non-malignant prostate tissue, adenocarcinoma and percentage of fibrosis.

The TULSA procedure has also been described previously in Chin et al [26]. Briefly, the therapeutic ultrasound applicator (UA, Fig. 1) of the TULSA-PRO device (Profound Medical Inc., Toronto, ON, Canada) is inserted into the prostate through the urethra of an anaesthetised patient, and the

Table 1 MRI sequences

Purpose	Sequence	Orientation	TE/TR	FOV	Acq. Matrix	Slice Thick./Gap	# Avg
Image sequences used during MRI-guided TULSA procedure							
Treatment Planning	T2w Turbo Spin Echo	2D Oblique Axial, Sagittal and Coronal	51/4,500 ms	260 x 260 mm	256 x 256	2.5/0 mm	1
Real-Time Thermometry	Echo Planar Imaging	2D Oblique Axial	8/350 ms	260 x 260 mm	128 x 128	4.0/1.0 mm	1
Post-Treatment Contrast Enhanced Imaging	Fast Low Angle Shot (FLASH) Gradient Echo	3D Oblique Axial	2.46/20 ms	234 x 234 mm	256 x 256	5.0/0 mm	2
Image sequences used for prostate volume reduction analysis							
Treatment-day Anatomical (CAN/USA)	T2w Turbo Spin Echo	2D Oblique Axial	111/5,120 ms	260 x 260 mm	384 x 384	2.5/2.5 mm	4
Treatment-day Anatomical (Germany)	T2w Turbo Spin Echo	2D Oblique Axial	91/5,550 ms	230 x 195 mm	320 x 272	3.0/0 mm	2
12-month Anatomical (CAN/USA)	T2w Turbo Spin Echo	2D Axial	101/3,800 ms	200 x 200 mm	320 x 320	3.0/0.3 mm	4
12-month Anatomical (Germany)	T2w Turbo Spin Echo	2D Axial	146/8,000 ms	200 x 200 mm	768 x 768	3.0/0.3 mm	2

patient is advanced into the MRI. A robotic positioning system holds and translates the UA for MRI-guided alignment with the targeted prostate tissue. T2w images are used to prescribe target boundaries for each element. Ultrasound ablation of the target volume is delivered in a continuous 360° rotation of the UA under real-time MR-t guidance and control, where each of the ten 5-mm elements emits directional, but not focused, high-intensity ultrasound directly into the adjacent prostate. During energy delivery, segmented echo-planar images (EPI) are acquired dynamically (12 images every 5.9 s; Table 1) and used to calculate MR-t by the proton resonance frequency shift method [21]. MR-t is immediately displayed (Fig. 2) and used by a feedback algorithm to adjust the frequency and power of each UA element, and the rate at which the positioning system rotates the UA, thereby depositing heat according to the treatment plan. Post-treatment CE-MR images were acquired following weight-adjusted intravenous injection of standard institutional gadolinium-based contrast agent (0.1 mmol/kg).

Boundaries of the treatment plan prostate volume (PV_{TP}, Fig. 1D, red) were delineated in consensus by the attending urologist and board-certified radiologist on T2w oblique-axial MR images acquired transverse to the UA and aligned with each transducer element. In accordance with the investigative goals of safety and feasibility in this Phase I trial, the target prostate volume (TPV, Fig. 1D, cyan) boundary was defined with a 3-mm margin inside the PV_{TP} prostate boundary. The TPV was the intended extent of immediately lethal ≥ 55 °C heating defining the ATAV [24, 25, 27]. The 3-mm margin allows assessment of the extent of post-interventional delayed cellular necrosis beyond the ATAV. Delayed necrosis is expected to correspond with the DTAV, defined by a thermal isoeffective dose [28] of at least 240 cumulative equivalent minutes at 43 °C (CEM43), a widely accepted predictor of the extent of thermal coagulation [29, 30]. DTAV has not been reported for patients undergoing TULSA, but based on preclinical data and validated simulations [31–33], DTAV was expected to extend 1.3 ± 0.5 mm (maximum 3 mm) past the ATAV for a predicted 10 ± 3% sparing of residual viable prostate tissue along the gland's periphery [26]. Figure 2 illustrates the calculation of acute and delayed ablation volumes from intraprocedural MR-t.

Central radiology assessment

Central radiology (CR) review was performed at the German Cancer Research Centre (DKFZ, Heidelberg, Germany) using customized semi-automatic contouring software by the MEVIS Fraunhofer Institute, based on MeVisLab (MeVis Medical Solutions AG, Bremen, Germany) [34] and the medical imaging toolkit (MITK, www.mitk.org) [35]. Prostate

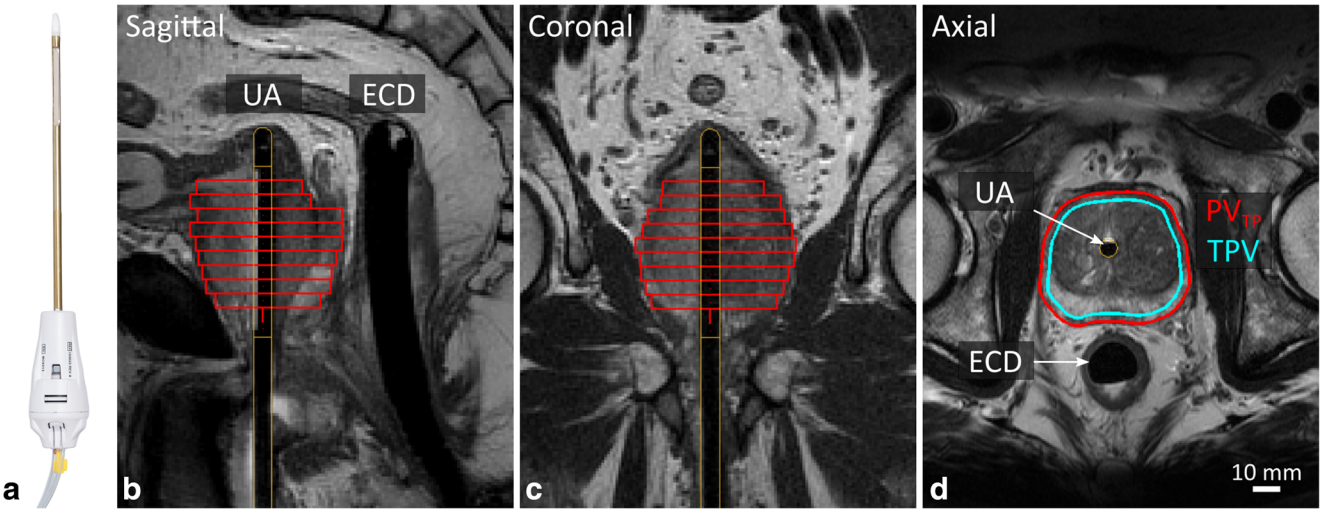

Fig. 1 TULSA device, image-based positioning and therapy planning. (**a**) Photograph of the transurethral therapeutic ultrasound applicator (UA), which incorporates a linear array of ten independent ultrasound transducers that emit directional, but not focused, high-intensity ultrasound energy directly into the adjacent prostate. (**b-d**) Sagittal (**b**), coronal (**c**) and axial (**d**) T2-weighted images used for treatment planning demonstrate the UA after it was advanced to its treatment position using the linear motion of the robotic positioning system. A passive endorectal cooling device (ECD) thermally protects the rectum. Using the treatment delivery console, boundaries of the treatment plan prostate volume (PV_{TP}, D, red) were delineated in consensus by the attending urologist and board-certified radiologist on high-resolution T2w oblique-axial MR images acquired transverse to the UA and aligned with each ultrasound transducer element. In accordance with the investigative goals of the Phase 1 trial, the target prostate volume (TPV, D, cyan) boundary was defined with a 3-mm margin inside the PV_{TP} prostate boundary, and targeted to 55 °C for complete immediate ablation

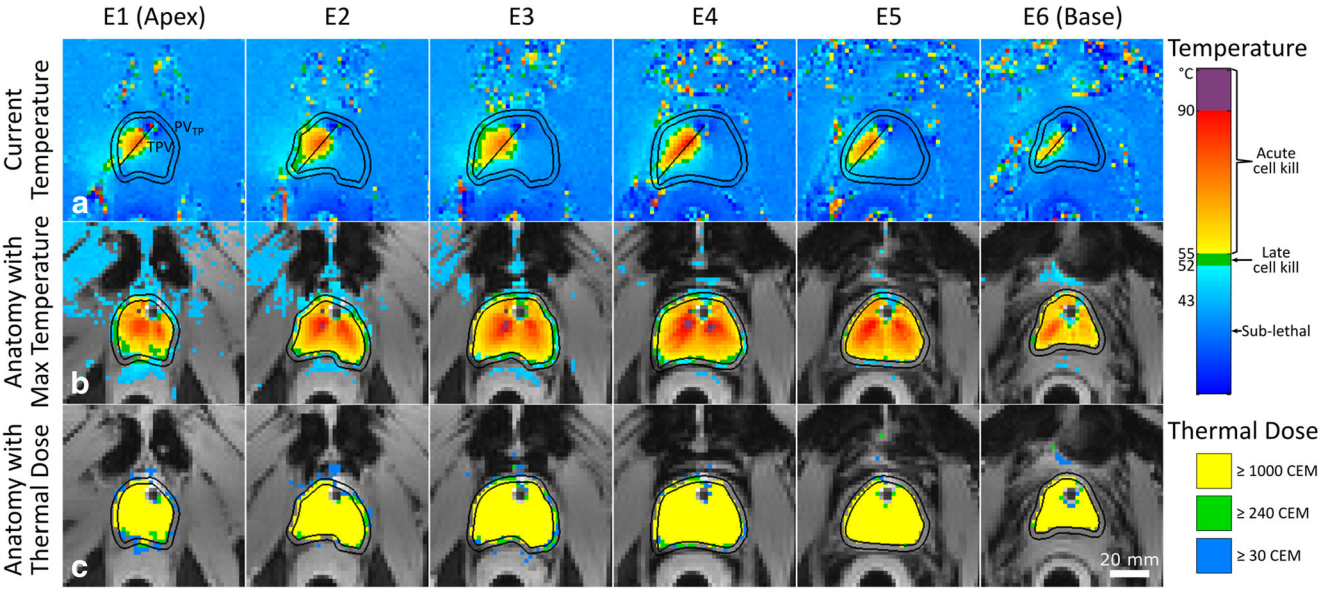

Fig. 2 Calculation of acute and delayed ablation volumes from intra-procedural MR temperature mapping. Real-time MR temperature mapping for a 65-year-old patient with Gleason 6 prostate cancer, initial PSA of 4.98 ng/ml and 12-month PSA of 0.2 ng/ml. During treatment, EPI images in 12 axial planes covering the ten transducer elements and adjacent slices are acquired every 5.9 s, and immediately used to calculate temperature maps in the prostate and surrounding tissue for automated feedback control and for display to the treating physician. **Top row:** Current temperature distribution at one time point during treatment, on the 6 planes where heat was actively delivered, with ultrasound propagation in the direction indicated by the black line. Outer black overlay indicates prostate boundary delineated by treating radiologist (PV_{TP}), inner black overlay indicates target boundary (TPV) defined by a 3-mm safety margin within the prostate boundary. **Middle row:** Cumulative maximum temperature for the completed treatment, with temperatures above 43 °C overlaid on the corresponding magnitude EPI image. The acute thermal ablation volume (ATAV, 55 °C isotherm) is represented by the green to yellow transition in the temperature colour scale. **Bottom row:** Thermal dose above 30 cumulative equivalent minutes at 43 °C (CEM43) overlaid on the magnitude EPI image. The delayed thermal ablation volume (DTAV, 240 CEM43 isocontour) is represented by the transition from blue to green in the thermal dose colour scale

volume (PV) and non-perfused volume were measured using T2w and subtracted CE-MRI on treatment day (PV_0, NPV_{IPT}) and at 12 months (PV_{12M}, NPV_{12M}). DTAV was calculated from the MR-t maps inside the 240 CEM43 isocontours. These metrics were compared with treatment plans and previously reported ATAV (volume bounded by the 55 °C isotherm of MR-t).

Statistical analysis

Residual volume of viable prostate tissue at 12 months was measured as the remaining prostate volume (PV_{12M}) less the non-perfused volume at 12 months within the PV_{12M} (NPV_{12M}), scaled by the fraction of fibrosis in biopsy cores (F) to account for the expected presence of enhancing fibrous tissue [36, 37]: (1-F) * ($PV_{12M} - NPV_{12M}$).

Using treatment-day MRI and MR-t data, the predicted reduction of viable prostate tissue volume based on thermal dose is the fraction of prostate volume covered by the DTAV: (DTAV ∩ PV_{TP}) / PV_{TP}. Likewise, the predicted reduction based on non-perfused volume is the fraction of prostate volume covered by the NPV_{IPT}: (NPV_{IPT} ∩ PV_{TP}) / PV_{TP}. Differences in reduction between MR-t and NPV estimates versus 12-month measurements were assessed using paired t-tests.

Agreement between treatment-day volumetric contours of NPV, DTAV and ATAV was assessed according to the following three definitions: (a) linear accuracy and precision, defined as in Chin et al [26] by the mean and standard deviation (SD) of the distance between intended and measured boundaries sampled at 1° polar increments; (b) volumetric over- and under-targeting; and (c) region overlap measured by the Dice Similarity Coefficient (DSC) [38].

Summary statistics are represented by the median and inter-quartile range (IQR). PV measurements based on site-specific treatment plans (PV_{TP}) and CR assessment (PV_0) were compared using correlation (R^2) and DSC.

Results

Delayed compared to acute ablation volume and non-perfused volume

Comparison of treatment-day metrics of ablation accuracy is presented in Table 2. DTAV exceeded ATAV by a median volume of 10 cc (132% of ATAV), extending 2.0–2.4 mm

Table 2 Thermal ablation accuracy on treatment day (n=30)

Treatment-day ablation parameters	Metric	Median (IQR)		
Treatment time (ultrasound ablation time)*		36 (26–44) min		
Prostate volume according to treatment plan*	PV_{TP}	44 (38–48) cc		
Target prostate volume (3-mm peripheral margin excluded)	TPV	31 (27– 34) cc		
Acute thermal ablation volume (within 55 °C isotherm on MR-t)	ATAV	31 (27–34) cc		
Delayed thermal ablation volume (within 240 CEM43 thermal dose isocontour on MR-t)	DTAV	42 (37–46) cc		
Immediate post-treatment non-perfused volume (Hypo-Intense on contrast-enhanced MRI)	NPV_{IPT}	19 (15–26) cc		
Comparison of metrics Median (IQR)	Spatial control of thermal ablation within target boundary: ATAV to TPV	Extent of delayed thermal ablation within prostate volume: DTAV to PV_{TP}	CE-MRI for assessment of acute treatment accuracy: NPV_{IPT} to ATAV	CE-MRI for assessment of delayed treatment effect: NPV_{IPT} to DTAV
Ratio	99 (95–104) %	96 (92 –98) %	64 (58–79) %	49 (40–62) %
Linear agreement accuracy	0.1 (-0.3–0.4) mm*	-0.3 (-0.7–0.0) mm	-2.5 (-3.5– -1.8) mm	-4.7 (-6.2– -4.2) mm
Linear agreement precision	1.3 (1.0–1.5) mm*	1.7 (1.5–2.1) mm	3.3 (2.6–4.3) mm	3.7 (3.2–4.6) mm
Over-estimated volume	0.6 (0.4–1.0) cc	1.5 (0.6–2.2) cc	0.6 (0.3–1.2) cc	0.1 (0.1–0.5) cc
Under-estimated volume	0.9 (0.2–1.3) cc	1.9 (1.3–3.4) cc	8.1 (5.9–11) cc	15 (12–22) cc
Dice similarity coefficient	0.94 (0.93–0.95)	0.92 (0.91–0.93)	0.78 (0.72–0.84)	0.70 (0.61–0.75)
Correlation (R^2)	0.98	0.98	0.74	0.69

IQR inter-quartile range

*Previously reported by Chin et al [26]

beyond the ATAV. NPV_{IPT}, an indicator of acute necrosis [33], was correlated to ATAV and DTAV, but systematically smaller by median distances of 2.5 and 4.7 mm. In addition to the previously assessed linear targeting accuracy and precision of 0.1 ± 1.3 mm between ATAV and TPV [26], median over- and under-targeted volumes were 0.6 ml and 0.9 ml, the median ratio of ATAV to TPV was 99%, and the median DSC was 0.94 indicating a high degree of congruence, concordant with the linear assessment. Examples of the spatial control boundaries are shown in two different patients in Fig. 3A and B.

Prostate volume reduction

Calculation of prostate volume reduction on 12-month follow-up imaging is given in Table 3, together with volume reduction predicted by treatment day thermal dose (DTAV) and NPV_{IPT}. The calculated residual viable prostate volume at 12 months corrected for fibrosis was 4.8 ml (2.3–8.4 ml), representing 12% (5–17%) of the baseline volume PV_0. This corresponded to a reduction of viable tissue volume at 12 months of 88% (83–95%). DTAV predicted a median (IQR) prostate volume reduction of 90% (87–92%), while NPV_{IPT} predicted a reduction of 53% (43–57%). As demonstrated in Fig. 4, the median difference between the DTAV prediction and the measured reduction at 12 months was +3.7 cc (IQR -5 to +7 cc); a paired t-test was not significant ($p = 0.12$). Between the NPV_{IPT} prediction and the measured reduction there was a larger difference of -17 cc (-23 to -13 cc); the paired t-test was highly significant ($p < 0.0001$).

Baseline prostate volume measurements

Repeatability was high between baseline PV measurements performed on treatment day by the local radiologist (PV_{TP}) and blinded retrospective assessment performed during central radiology review (PV_0), with R^2 of 0.77, median DSC of 0.89, volume ratio of 100% and absolute difference of 0.0 ml.

Discussion

This study extends the published clinical outcomes of the Phase I TULSA trial [26] by presenting (a) a quantitative analysis of prostate volume reduction based on the morphological 12-month follow-up MRI data corrected for fibrosis, and (b) a quantitative assessment of the relationship of

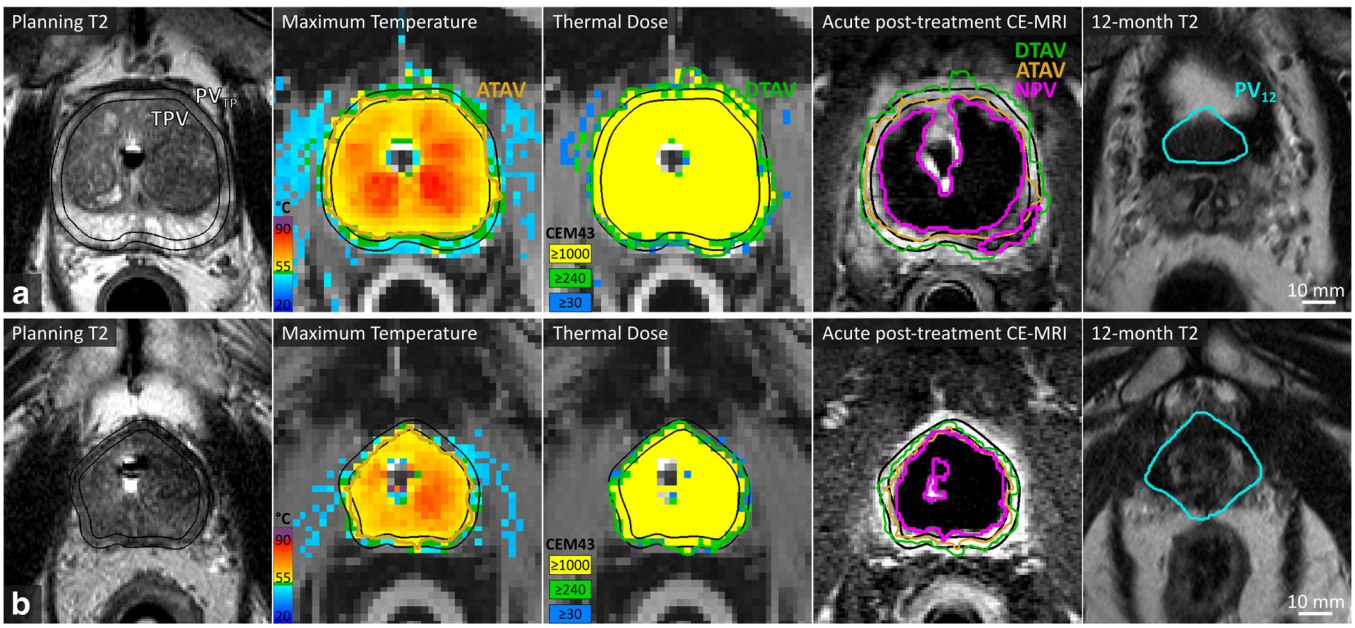

Fig. 3 Synopsis of treatment plan, temperature monitoring, ablative metrics and 12-month follow-up. Images from two patients: (**a**) A 69-year-old patient with Gleason 6 prostate cancer, initial PSA of 8.41 ng/ml and 12-month PSA of 0.7 ng/ml; (**b**) a 70-year-old patient with Gleason 6 prostate cancer, initial PSA of 7.49 ng/ml and 12-month PSA of 0.7 ng/ml. From left to right: boundaries of target prostate volume (TPV) and overall prostate volume (PV_{TP}) superimposed on axial T2-weighted planning images (left panels). Maximum temperature maps demonstrate that the acute thermal ablation volume (ATAV, orange) closely matches the TPV (second panels from the left). Thermal dose maps show a close match of delayed thermal ablation volume (DTAV, 240 CEM43 isotherm, green) and prostate boundary (middle panel). DTAV (green), ATAV (orange) and non-perfused volume (NPV, magenta) contours are overlaid on subtracted acute post-treatment contrast enhanced T1-weighted (CE-MRI) images, together with TPV and PV_{TP} (black) for direct comparison (second panels from the right). Twelve-month prostate volume contours (PV_{12}, cyan) are overlaid on 12-month follow-up T2-weighted axial images (right panels)

Table 3 Prostate volume reduction at 12 months (n=29)

Parameter	Equation	Median (IQR)
Treatment day predictors of 12-month prostate volume reduction		
DTAV-predicted prostate volume reduction (cc)	$DTAV \cap PV_{TP}$	39 (35–41) cc
DTAV-predicted residual prostate volume (% of baseline)	$1–(DTAV \cap PV_{TP} / PV_{TP})$	10 (8–13) %
DTAV-predicted prostate volume reduction (% of baseline)	$DTAV \cap PV_{TP} / PV_{TP}$	90 (87–92) %
NPV-predicted prostate volume reduction (cc)	$NPV_{IPT} \cap PV_{TP}$	20 (16–28) cc
NPV-predicted prostate volume reduction (% of baseline)	$NPV_{IPT} \cap PV_{TP} / PV_{TP}$	53 (43–57) %
12-Month prostate volume reduction – central radiologist		
Baseline prostate volume	PV_0	43 (39–47) cc
12-Month prostate volume (incl. NPV and fibrosis)	PV_{12M}	21 (18–24) cc
12-month NPV	NPV_{12M}	9 (6–12) cc
12-month Perfused Volume (incl. fibrosis)	$PV_{12M}–NPV_{12M}$	11 (7.7–13) cc
12-month estimated fibrosis from biopsy cores	F	54 (31–67) %
12-month residual prostate volume	$(1-F)* (PV_{12M}–NPV_{12M})$	4.8 (2.3–8.4) cc
12-month residual prostate volume (% of baseline)	$(1-F)* (PV_{12M}–NPV_{12M}) / PV_0$	12 (5–17) %
Prostate volume reduction based on 12-month imaging follow-up (cc)	$PV_0–(1-F)* (PV_{12M}–NPV_{12M})$	38 (31–45) cc
Prostate volume reduction based on 12-month imaging follow-up (% of Baseline)	$1–(1-F)* (PV_{12M}–NPV_{12M}) / PV_0$	88 (83–95) %
Inter-radiologist repeatability		
Ratio of baseline prostate volume, central radiologist to treatment plan	PV_0 / PV_{TP}	100 (87–107) %
Difference in baseline prostate volume, central radiologist to treatment plan	$PV_0–PV_{TP}$	0.0 (-5.8–2.7) cc
Dice similarity coefficient		0.89 (0.87–0.90)
Correlation (R^2)		0.77

IQR inter-quartile range

immediate non-perfused volume and MR-t derived expected ablation volume (DTAV) to measured tissue ablation at 12 months.

Important insights can be gained by examining these additional factors. MRI-guided TULSA achieved an 88% reduction of viable prostate tissue volume at 12 months, in excellent agreement with the expected ablation volume given by thermal dose calculated from MR-t. This validates the median 10% tissue sparing at the periphery predicted by simulations. DTAV extended 2.0 – 2.4 mm beyond the ATAV and had close agreement with the PV_{TP}, quantifying the margin of delayed tissue ablation beyond the target boundary in individual patients, and confirming the appropriateness of the 3-mm safety margin mandated in this safety and feasibility study. These results affirm the thermal cellular ablation relationships of previous preclinical and treat-and-resect clinical studies of TULSA [24, 25, 27, 30] and support their use in subsequent studies with more aggressive treatment margins.

NPV qualitatively appeared to follow the target boundary, but quantitative analysis demonstrated a systematic underestimation of tissue ablation. Non-perfused volume on immediate post-treatment contrast-enhanced MRI represented only 64% of the ATAV, and predicted an only 53% reduction in viable prostate tissue volume at 12 months. This is anticipated by previous treat-and-resect studies: in pre-clinical experiments with histological correlation [33], the ablation boundary fell within the haemorrhagic zone of hyper-enhancement surrounding the NPV_{IPT}, and the NPV_{IPT} underestimated the extent of acute tissue necrosis by 1–4 mm, compatible with the 1.8- to 3.5-mm underestimation of the ATAV observed in our study. As such, use of the DTAV appears preferable for the prediction of tissue ablation compared to NPV, while NPV provides functional

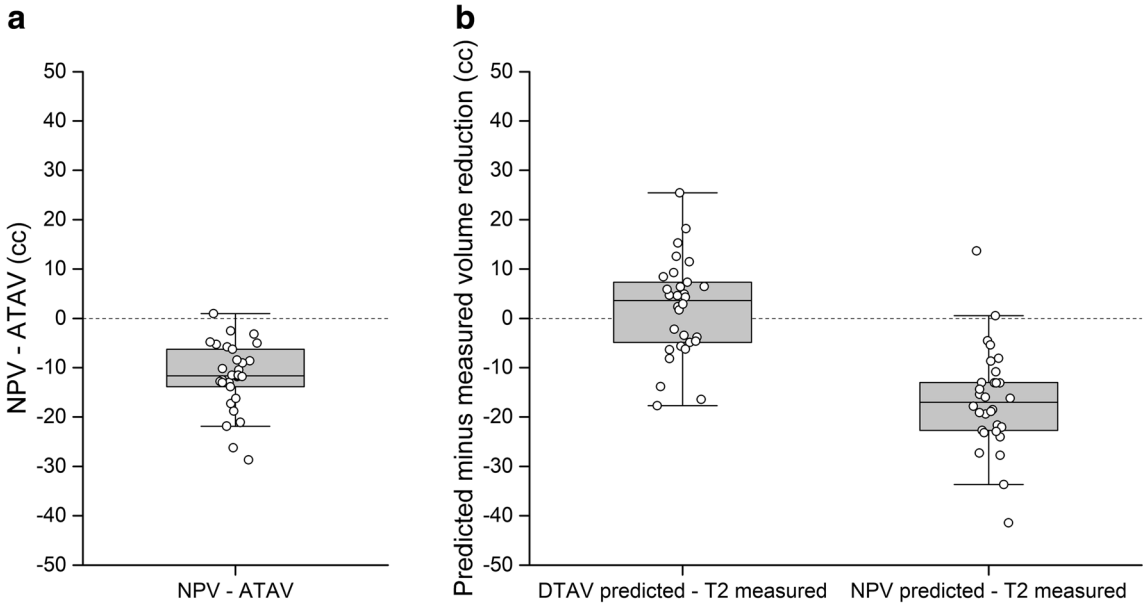

Fig. 4 Comparison of volumetric prostate metrics. Box plots of the difference between volumetric prostate metrics, comparing metrics available on treatment day (**a**), and comparing treatment-day NPV and DTAV as predictors of the 12-month volumetric assessment (**b**). NPV is systematically smaller than ATAV (**a**). Measured viable prostate volume reduction at 12 months is in good agreement with volume reduction predicted by MR-thermometry based DTAV (**b**, left), while it is systematically underestimated by immediate post-treatment NPV (**b**, right)

confirmation that conformal ablation has been achieved independent from MR-t.

Additional accuracy metrics, including DSC and volumetric over- and underestimation, closely followed the linear assessment used for ATAV in the initial publication, confirming the validity of these analyses for the newly examined volumes. As an internal control, treatment-day volumetry was in excellent agreement between on-site and central radiology assessment, a mandatory precondition for successful comparison of the derived metrics.

A strength of this study is patient-specific correction of imaging-based measurements of volume reduction by fibrosis fractions determined from biopsy cores at a central laboratory. Previous studies of post-ablation prostate histopathology at time points beyond 1 year have shown stromal fibrosis as the most common finding in non-tumour post-HIFU biopsy tissue; coagulative necrosis is less common and diminishes with the progressive resorption of necrotic tissue over time; varying amounts of acute, chronic or granulomatous inflammation are found [36, 37]. Therefore, for precise assessment of residual viable prostate tissue, it is important to account for space-occupying predominantly fibrotic remnants of successfully treated tissue. Viable PV reduction of 88% reported here is in accordance with early treatment effectiveness based on biochemical assessment evaluated by Chin et al, who reported a 12-month PSA of 0.8 ng/ml, representing a reduction of 86% (72–92%) from pre-treatment baseline values [26].

This study has several limitations. Assessment of tissue necrosis was based primarily on imaging criteria, and not directly correlated to histology; however, previous treat-and-resect studies of MRI-guided TULSA describe the relationships between imaging and histology used as the basis for this Phase I study [25, 27]. The assessment of fibrosis may be limited by biopsy sampling bias, and fibrosis assessment at 12 months may underestimate treatment effect if fibrosis has been replaced by interval tumour growth, factors that may have influenced the volumetric calculations. Here, histopathological sections could not be obtained because long-term follow-up without radical prostatectomy was necessary to assess safety and secondary outcomes including quality of life and oncological efficacy.

Conclusion

Quantitative assessment of treatment-day and 12-month follow-up MR imaging from the Phase I study of MRI-guided TULSA indicate a 12-month fibrosis-corrected viable prostate volume reduction of 88%. The MR-thermometry based 240 cumulative equivalent minute thermal dose volume (DTAV) was identified as a useful predictor of measured prostate volume reduction. Conversely, non-perfused volume calculated from immediate post-treatment CE-MRI systematically underestimated both ATAV and the measured volume reduction. As predicted by previous simulations, per-patient quantitative assessment confirmed a median 10% of untreated peripheral viable prostate tissue volume remaining after treatment, both explaining residual disease on

follow-up and supporting an extension of the treatment boundary in the ongoing pivotal study.

Funding This study has received funding by Profound Medical Inc.

Compliance with ethical standards

Guarantor The scientific guarantor of this publication is Heinz-Peter Schlemmer.

Conflict of interest David Bonekamp is speaker for Profound Medical Inc.

Mathieu Burtnyk is director of clinical affairs of Profound Medical Inc. with a salary and stock options.

Robert Staruch is senior clinical scientist at Profound Medical Inc., with a salary and stock options.

Jason M. Hafron declares: Amgen-paid speaker, Armune Biosciences Inc, advisory board/paid speaker, Dendreon-Advisory Board, paid speaker, Myriad, and paid speaker, United Physicians- Board of directors

Heinz-Peter Schlemmer declares: Consulting fee or honorarium: Siemens, Curagita, Profound, Bayer. Travel support: Siemens, Curagita, Profound, Bayer. Board Member: Curagita. Consultancy: Curagita, Bayer. Grants/Grants pending: BMBF, Deutsche Krebshilfe, Dietmar-Hopp-Stiftung, Roland-Ernst-Stiftung. Payment for lectures: Siemens, Curagita, Profound, Bayer.

Boris Hadaschik declares: Personal fees: Janssen, BMS, Astrellas, Bayer. Grants: Janssen, Astrellas, BMS, German Cancer Aid, German Research Foundation.Grant: Profound Medical.

Gencay Hatiboglu declares: Consultancy for BMS.

Timur Kuru has nothing to declare.

James Relle has nothing to declare.

Maya Mueller-Wolf has nothing to declare.

Matthias Röthke declares consulting fee and payment for lectures: Siemens Healthineers, Curagita AG.

Sascha Pahernik reports personal fees from Bayer, personal fees from Astellas, personal fees from Janssen, outside the submitted work.

Valentin Popeneciu has nothing to declare.

Joseph Chin declares: Investigator and consultant for Profound Medical Inc., US HIFU, Endocare; Paid Advisory Board/Consultancy for Abbvie, Johnson & Johnson/Janssen, Amgen, Tersera, Novartis, Astellas, Bayer, Sanofi-Aventis.

Michele Billia has nothing to declare.

Kiran Nandalur has nothing to declare.

Markus Hohenfellner has nothing to declare.

Statistics and biometry No complex statistical methods were necessary for this paper.

Informed consent Written informed consent was obtained from all subjects (patients) in this study.

Ethical approval Institutional Review Board approval was obtained.

Study subjects or cohorts overlap Some study subjects or cohorts have been previously reported in Chin JL, Billia M, Relle J, et al. Magnetic resonance imaging-guided transurethral ultrasound ablation of prostate tissue in patients with localized prostate cancer: a prospective Phase 1 clinical trial. Eur Urol. 2016;70(3):447–455.

Methodology
- prospective
- experimental
- multicentre study

References

1. Siegel RL, Miller KD, Jemal A (2016) Cancer statistics, 2016. CA Cancer J Clin 66(1):7–30
2. Albertsen PC (2005) 20-Year Outcomes Following Conservative Management of Clinically Localized Prostate Cancer. JAMA 293(17):2095
3. Resnick MJ, Koyama T, Fan K-H et al (2013) Long-Term Functional Outcomes after Treatment for Localized Prostate Cancer. N Engl J Med 368(5):436–445
4. Tosoian JJ, Mamawala M, Epstein JI et al (2015) Intermediate and longer-term outcomes from a prospective active-surveillance program for favorable-risk prostate cancer. J Clin Oncol 33(30):3379–3385
5. Klotz L, Vesprini D, Sethukavalan P et al (2015) Long-term follow-up of a large active surveillance cohort of patients with prostate cancer. J Clin Oncol 33(3):272–277
6. Napoli A, Anzidei M, De Nunzio C et al (2013) Real-time magnetic resonance-guided high-intensity focused ultrasound focal therapy for localised prostate cancer: Preliminary experience. Eur Urol 63(2):395–398
7. Mendez H, Passoni Maria N, Pow-Sang J, Jones Stephen J, Polascik J (2015) Comparison of Outcomes Between Preoperatively Potent Men Treated with Focal Versus Whole Gland Cryotherapy in a Matched Population. J Endourol 29(10):1193
8. Azzouzi AR, Barret E, Moore CM et al (2013) TOOKAD® Soluble vascular-targeted photodynamic (VTP) therapy: Determination of optimal treatment conditions and assessment of effects in patients with localised prostate cancer. BJU Int 112(6):766–774
9. Lepor H, Llukani E, Sperling D, Fütterer JJ (2015) Complications, Recovery, and Early Functional Outcomes and Oncologic Control Following In-bore Focal Laser Ablation of Prostate Cancer. Eur Urol 68(6):924–926
10. Murray KS, Ehdaie B, Musser J et al (2016) Pilot Study to Assess Safety and Clinical Outcomes of Irreversible Electroporation for Partial Gland Ablation in Men with Prostate Cancer. J Urol. United States 196(3):883–890
11. Cosset JM, Cathelineau X, Wakil G et al (2013) Focal brachytherapy for selected low-risk prostate cancers: A pilot study. Brachytherapy 12(4):331–337
12. Zlotta AR, Djavan B, Matos C et al (1998) Percutaneous transperineal radiofrequency ablation of prostate tumour: safety, feasibility and pathological effects on human prostate cancer. Br J Urol 81(2):265–275
13. Chen JC, Moriarty JA, Derbyshire JA et al (2000) Prostate Cancer: MR Imaging and Thermometry during Microwave Thermal Ablation-Initial Experience. Radiology 214(1):290–297
14. Valerio M, Cerantola Y, Eggener SE et al (2016) New and Established Technology in Focal Ablation of the Prostate: A Systematic Review. Eur Urol 71(1):17–34. https://doi.org/10.1016/j.eururo.2016.08.044
15. Feijoo ERC, Sivaraman A, Barret E et al (2016) Focal High-intensity Focused Ultrasound Targeted Hemiablation for Unilateral Prostate Cancer: A Prospective Evaluation of Oncologic and Functional Outcomes. Eur Urol 69(2):214–220. https://doi.org/10.1016/j.eururo.2015.06.018
16. Radtke JP, Wiesenfarth M, Kesch C et al (2017) Combined Clinical Parameters and Multiparametric Magnetic Resonance Imaging for Advanced Risk Modeling of Prostate Cancer-Patient-tailored Risk Stratification Can Reduce Unnecessary Biopsies. Eur Urol. https://doi.org/10.1016/j.eururo.2017.03.039
17. Radtke JP, Kuru TH, Bonekamp D et al (2016) Further reduction of disqualification rates by additional MRI-targeted biopsy with transperineal saturation biopsy compared with standard 12-core

systematic biopsies for the selection of prostate cancer patients for active surveillance. Prostate Cancer Prostatic Dis 19(3):283–291
18. Valerio M, Donaldson I, Emberton M et al (2015) Detection of clinically significant prostate cancer using magnetic resonance imaging-ultrasound fusion targeted biopsy: A systematic review. Eur Urol 68(1):8–19
19. Ahmed HU, El-Shater Bosaily A, Brown LC et al (2017) Diagnostic accuracy of multi-parametric MRI and TRUS biopsy in prostate cancer (PROMIS): a paired validating confirmatory study. Lancet 389(10071):815–822
20. Siddiqui MM, Rais-Bahrami S, Turkbey B et al (2016) Comparison of MR/Ultrasound Fusion–Guided Biopsy With Ultrasound-Guided Biopsy for the Diagnosis of Prostate Cancer. JAMA 1210(4):390–397
21. Ishihara Y, Calderon A, Watanabe H et al (1995) A precise and fast temperature mapping using water proton chemical shift. Magn Reson Med 34(6):814–823
22. Ghai S, Louis AS, Van Vliet M et al (2015) Real-time MRI-guided focused ultrasound for focal therapy of locally confined low-risk prostate cancer: Feasibility and preliminary outcomes. Am J Roentgenol 205(2):W177–W184
23. Eggener SE, Yousuf A, Watson S, Wang S, Oto A (2016) Phase II Evaluation of Magnetic Resonance Imaging Guided Focal Laser Ablation of Prostate Cancer. J Urol. United States 196(6):1670–1675
24. Chopra R, Tang K, Burtnyk M et al (2009) Analysis of the spatial and temporal accuracy of heating in the prostate gland using transurethral ultrasound therapy and active MR temperature feedback. Phys Med Biol 54(9):2615–2633
25. Ramsay E, Mougenot C, Staruch R et al (2017) Evaluation of Focal Ablation of Magnetic Resonance Imaging Defined Prostate Cancer Using Magnetic Resonance Imaging Controlled Transurethral Ultrasound Therapy with Prostatectomy as the Reference Standard. J Urol 197(1):255–261
26. Chin JL, Billia M, Relle J et al (2016) Magnetic Resonance Imaging–Guided Transurethral Ultrasound Ablation of Prostate Tissue in Patients with Localized Prostate Cancer: A Prospective Phase 1 Clinical Trial. Eur Urol 70(3):447–455
27. Chopra R, Colquhoun A, Burtnyk M et al (2012) MR imaging-controlled transurethral ultrasound therapy for conformal treatment of prostate tissue: initial feasibility in humans. Radiology 265(1):303–313
28. Sapareto SA, Dewey WC (1984) Thermal dose determination in cancer therapy. Int J Radiat Oncol Biol Phys 10(6):787–800
29. McDannold NJ, King RL, Jolesz FA, Hynynen KH (2000) Usefulness of MR imaging-derived thermometry and dosimetry in determining the threshold for tissue damage induced by thermal surgery in rabbits. Radiology 216(11):517–523
30. Burtnyk M, Hill T, Cadieux-Pitre H, Welch I (2015) Magnetic resonance image guided transurethral ultrasound prostate ablation: a preclinical safety and feasibility study with 28-day followup. J Urol 193(5):1669–1675
31. Burtnyk M, N'Djin WA, Kobelevskiy I, Bronskill M, Chopra R (2010) 3D conformal MRI-controlled transurethral ultrasound prostate therapy: validation of numerical simulations and demonstration in tissue-mimicking gel phantoms. Phys Med Biol. England 55(22):6817–6839
32. Burtnyk M, Chopra R, Bronskill M (2010) Simulation study on the heating of the surrounding anatomy during transurethral ultrasound prostate therapy: a 3D theoretical analysis of patient safety. Med Phys 37(6):2862–2875
33. Boyes A, Tang K, Yaffe M, Sugar L, Chopra R, Bronskill M (2007) Prostate Tissue Analysis Immediately Following Magnetic Resonance Imaging Guided Transurethral Ultrasound Thermal Therapy. J Urol 178(3):1080–1085
34. Ritter BF, Boskamp T, Homeyer A et al (2011) Medical Image Analysis: A Visual Approach. IEEE Pulse 2(6):60–70
35. Nolden M, Zelzer S, Seitel A et al (2013) The medical imaging interaction toolkit: Challenges and advances: 10 years of open-source development. Int J Comput Assist Radiol Surg 8(4):607–620
36. Biermann K, Montironi R, Lopez-Beltran A, Zhang S, Cheng L (2010) Histopathological findings after treatment of prostate cancer using high-intensity focused ultrasound (HIFU). Prostate 70(11):1196–1200
37. Ryan P, Finelli A, Lawrentschuk N et al (2012) Prostatic needle biopsies following primary high intensity focused ultrasound (HIFU) therapy for prostatic adenocarcinoma: histopathological features in tumour and non-tumour tissue. J Clin Pathol 65(8):729–734
38. Dice LR (1945) Measures of the Amount of Ecologic Association Between Species. Ecology 26(3):297–302